Lateral diffusivity of lipid analogue excimeric probes in dimyristoylphosphatidylcholine bilayers

Massimo Sassaroli, Matti Vauhkonen,* Douglas Perry, and Josef Eisinger
Department of Physiology and Biophysics, Mount Sinai School of Medicine, New York 10029; and *Department of Medicine, Albert Einstein College of Medicine, Bronx, New York 10461

ABSTRACT The lateral mobility of pyrenyl phospholipid probes in dimyristoylphosphatidylcholine (DMPC) vesicles was determined from the dependence of the pyrene monomeric and excimeric fluorescence yields on the molar probe ratio. The analysis of the experimental data makes use of the milling crowd model for two-dimensional diffusivity and the computer simulated random walks of probes in an array of lipids. The fluorescence yields for 1-palmitoyl-2-(1'-pyrenedecanoyl)phosphatidylcholine ($py_{10}PC$) in DMPC bilayers are well fitted by the model both below and above the fluid-gel phase transition temperature (T_c) and permit the evaluation of the probe diffusion rate (f), which is the frequency with which probes take random steps of length L, the host membrane lipid–lipid spacing. The lateral diffusion coefficient is then obtained from the relationship $D = fL^2/4$. In passing through the fluid-gel phase transition of DMPC ($T_c = 24°C$), the lateral mobility of $py_{10}PC$ determined in this way decrease only moderately, while D measured by fluorescence photobleaching recovery (FPR) experiments is lowered by two or more orders of magnitude in gel phase. This difference in gel phase diffusivities is discussed and considered to be related either to (*a*) the diffusion length in FPR experiments being about a micrometer or over 100 times greater than that of excimeric probes (≈1 nm), or (*b*) to nonrandomicity in the distribution of the pyrenyl probes in gel phase DMPC. At 35°C, in fluid DMPC vesicles, the diffusion rate is $f = 1.8 \times 10^8\ s^{-1}$, corresponding to $D = 29\ \mu m^2\ s^{-1}$, which is about three times larger than the value obtained in FPR experiments. The activation energy for lateral diffusion in fluid DMPC was determined to be 8.0 kcal/mol.

INTRODUCTION

The dynamical properties of biological membranes play an important part in the diverse functions of cells, and a variety of physical techniques have been employed to obtain quantitative information about the fluidity of membranes and of their model systems. These include paramagnetic membrane probes (Sheats and McConnell, 1978), NMR of deuterated lipid (Kuo and Wade, 1979), and the use of fluorescence polarization probes (Davenport et al., 1986) like diphenylhexatriene (DPH). The lateral fluidity of membranes has been investigated primarily by fluorescence photobleaching recovery (FPR or FRAP) methods (Vaz et al., 1982), for which the characteristic diffusion distances are of the order of micrometers, because that is the minimum diameter of the bleached spot. Much shorter diffusion lengths, of the order of a few lipid–lipid spacings, obtain for the mobility of excimeric probes (Galla et al., 1979; Eisinger et al., 1986), whose root-mean-square diffusion distance is given by $2\sqrt{(D\tau_M)}$, where τ_M is the lifetime of the excited monomer ($\approx 10^{-7}$ s for pyrene) and D is the lateral diffusion coefficient.

This paper presents experimental protocols for determining the local lateral diffusivity of excimeric probes in a homogeneous bilayer system. The analysis of fluorometric titration experiments is based on a simple model for two-dimensional diffusivity, the so-called milling crowd model, and makes use of the results of computer-generated random migrations of excimeric probes. This model assumes that probes are randomly distributed in a homogeneous host membrane and was previously utilized to measure the mobility of pyrenedodecanoic acid probes in the membranes of intact erythrocytes (Eisinger et al., 1986). Like other biological membranes, the red cell membrane is heterogeneous, containing many species of phospholipids as well as a multitude of different membrane proteins with, on the average, only a few to tens of phospholipid molecules between them (Eisinger, 1989): as such it does not represent the ideal system for a critical evaluation of the model.

In the present investigation, the predictions of the milling crowd model are compared to the results of experiments performed with a homogeneous (i.e., single species) model membrane system. For this purpose the computer simulations of probe migration have been expanded and a nonlinear least squares fitting procedure was implemented for analyzing the experimental titrations. This methodology was used to determine the lateral mobility of pyrenyl phosphatidylcholine probes in unilamellar and multilamellar vesicles as a function of temperature, below and above the phase transition. While the

lateral fluidities measured by FPR and the present method are in acceptable agreement for fluid (liquid crystalline) DMPC bilayers, the short-range fluidity in the gel phase, as measured by the use of excimeric probes, is found to be considerably greater than that obtained by FPR experiments. This surprising result can be explained either by dislocation boundaries obstructing long-range diffusion or by a failure of the assumption that the excimeric probes are randomly distributed in gel DMPC, as required for the milling crowd model analysis.

An important motivation for investigating excimeric molecules as dynamic membrane probes is that they are well suited for measuring the spatial distribution of membrane fluidity. Thus, a membrane fluidity map may be created by combining the fluorescence microscopic images obtained at the monomeric and excimeric emission wavelengths. Because the diffusion length of excimeric probes is of the order of a few lipid–lipid spacings, they are suitable for mapping persistent heterogeneities in fluidity and membrane constitution with optical resolution ($\approx 0.2\ \mu m$). The existence and function of such lipid domains in membranes (Klausner and Kleinfeld, 1984) can therefore be investigated either by dynamic fluorescence spectroscopy (Davenport et al., 1986) or by quantitative fluorescence microscopy of single cells (Eisinger, 1989). Alternatively, intramolecular excimeric probes, which are discussed in a companion paper, may be used in a similar manner (Perry et al., 1988; Vauhkonen et al., 1990).

EXPERIMENTAL METHODS

All lipids were obtained from Avanti Polar Lipids, Birmingham, AL, and were dissolved in a chloroform/methanol (2:1) solvent (CM). Lipid stock solutions were prepared at concentrations of ~10 mM and their concentration was determined by the phosphate assay of Bartlett (1959). 1-Palmitoyl-2-(1'-pyrenedecanoyl)phosphatidylcholine ($py_{10}PC$) was obtained from Molecular Probes, Inc., Eugene, OR. The probes were dissolved in ethanol at concentrations of ~20 μM and their concentration was determined spectrophotometrically, using 42,000 cm^{-1} as the molar extinction coefficient of the pyrenyl moiety at 342 nm.

Small unilamellar vesicles (SUV) were prepared by the ethanolic injection technique of Kremer (Kremer et al., 1971), for which the authors report unilamellarity and a mean vesicular diameter of 40 nm when the SUV are prepared with a lipid concentration of ~5 mM. To prepare the SUVs, ~0.5 ml of the probe-lipid CM solution in the desired ratio was evaporated under a nitrogen stream; 50 μl of ethanol were added to rinse the walls of the vial and evaporated. After adding another 50 μl of ethanol, producing a final phospholipid concentration of ~2 mM, the vial was capped and vortexed. 20 μl of the solution were then injected into 2 ml of Hepes buffer (10 mM, pH 7.2, 140 mM NaCl, 5 mM KCl) using a constant rate syringe (Hamilton Co., Reno, NV). It is important that this step be taken using syringe and buffer at a temperature (35°C for DMPC) well above the gel-fluid transition temperature for the lipid.

Multilamellar vesicles (MLV) were prepared (Alecio et al., 1982) by evaporating the CM solution containing DMPC and $py_{10}PC$ in the desired ratio under a nitrogen stream. To eliminate any solvent residue, the dry mixture was then placed under vacuum for ~16 h. Hepes buffer was then added and the suspension was vortexed to produce MLVs. To obtain a more uniform vesicle size distribution, the MLV suspension was placed in an ultrasonic bath (Branson Inc., Danbury, CT; 100 W) at 35–40°C for 10 min.

Fluorescence measurements were made by use of an SLM-8000 steady-state spectrofluorometer (SLM Instruments, Inc., Urbana, IL), equipped with a thermostatically controlled 1-cm cuvette holder. Excitation and emission bandwidths were 4 nm and the excitation wavelength was 320 nm. Monomer and excimer emission intensities were measured at 378 and 480 nm, respectively. The absorption of the samples at the excitation wavelength was in all cases $<0.1\ cm^{-1}$. The average lifetime of the excited state of the isolated monomer, τ_M, was determined by use of a photon counting pulse fluorometer, using excitation picosecond pulses supplied by a mode-locked Nd-YAG-pumped dye laser.

After measuring their fluorescence spectra, the concentrations of pyrenyl probes in the samples were determined by adding to them aliquots of a 20% solution of deoxycholate (DOC) at 30°C, to provide a final DOC concentration of 1%. After the addition of the detergent, the fluorescence spectrum had the characteristic shape of purely monomeric emission, showing that the probes were well dispersed in the detergent micelles, and the intensity at 378 nm was used to determine the concentration of the pyrenyl probes by use of a calibration curve. The probe concentrations obtained in this way were within 10% of their nominal values and were reproducible to within 3%.

METHOD OF ANALYSIS

When an excited excimeric molecule (A*) is a nearest neighbor to one in its ground state (A), the two molecules may share the excitation energy and form an *excited dimer* or *excimer*. Because the fluorescence emitted by the monomer, A*, and the excimer, (AA)*, are usually well separated in energy, the emission spectrum of a solution containing excimeric probes is a sensitive function of probe concentration and diffusivity. Therefore, if the former is known, the second can be derived.

In this section we first describe a model-independent membrane fluidity parameter, x_0, and then show how absolute values of the probes lateral diffusion coefficient may be determined by use of a simple dynamic model.

Kinetic equations and the critical probe ratio

The kinetics of excimeric probes are described by the following equations:

$$A + A^* \underset{k_d}{\overset{K(x)}{\rightleftharpoons}} (AA)^* \qquad (1)$$

$$A^* \xrightarrow{k_M,\ k'_M} A + h\nu_M \qquad (2)$$

$$(AA)^* \xrightarrow{k_E,\, k'_E} 2A + h\nu_E \tag{3}$$

where $h\nu$ is the emitted photon, k and k' are the radiative and nonradiative deexcitation rates, and the subscripts M and E refer to monomeric and excimeric emissions. $K(x)$ is the concentration-dependent excimer formation rate, the probe concentration being expressed by x, the molar probe ratio:

$$x = \frac{[\text{probe}]}{[\text{probe}] + [\text{lipid}]}. \tag{4}$$

The monomer fluorescence quantum yield, $\Phi_M(x)$, remains constant as long as x is small and the excimer formation rate is negligible compared to the monomer deexcitation rate. At larger x values, $K(x)$ is comparable to $k_M + k'_M$ and the x-dependence of the monomer and excimer yields are given by

$$\Phi_M(x) = \frac{k_M}{k_M + k'_M + K(x)} \tag{5}$$

$$\Phi_E(x) = \frac{k_E}{k_E + k'_E} \frac{K(x)}{k_M + k'_M + K(x)} \tag{6}$$

$$r_\Phi(x) \equiv \Phi_E(x)/\Phi_M(x). \tag{7}$$

In deriving Eqs. 5 and 6 from the kinetic equations, the excimer dissociation rate, k_d, is assumed to be negligible compared with its deexcitation rate. If this is not the case, the corrected excimer formation rate is

$$K_{corr}(x) = \frac{k_E + k'_E + k_d}{k_E + k'_E} K(x). \tag{8}$$

It is useful to define Φ^*_M, the intrinsic monomer quantum yield for vanishingly small x ($K(x) \ll k_M + k'_M$) and Φ^*_E, the intrinsic excimer yield, which would obtain if an excimer were formed every time a monomer is excited (i.e., $K(x) \gg k_M + k'_M$)

$$\Phi^*_M = \frac{k_M}{k_M + k'_M} \tag{9}$$

$$\Phi^*_E = \frac{k_E}{k_E + k'_E} \tag{10}$$

$$r^*_\Phi \equiv \Phi^*_E/\Phi^*_M. \tag{11}$$

If τ_M is the lifetime of the isolated ($x \ll 1$) monomer,

$$\tau_M = (k_M + k'_M)^{-1}, \tag{12}$$

so that dividing Eqs. 5 and 6 by Eqs. 9 and 10, one obtains the following x-dependence of the quantum yields:

$$\Phi_M(x) = \Phi^*_M \frac{1}{1 + K(x)\,\tau_M} \tag{13}$$

$$\Phi_E(x) = \Phi^*_E \frac{1}{1 + [K(x)\,\tau_M]^{-1}}, \tag{14}$$

and, dividing Eq. 14 by 13,

$$r_\Phi(x)/r^*_\Phi = K(x)\,\tau_M. \tag{15}$$

At the critical probe ratio, x_0, the $K(x_0)$ is equal to the monomer decay rate, τ_M^{-1}, and

$$\Phi_M(x_0) = \Phi^*_M/2 \tag{16a}$$

$$\Phi_E(x_0) = \Phi^*_E/2 \tag{16b}$$

$$r^*_\Phi = r_\Phi(x_0). \tag{16c}$$

Eq. 16c is important because with it one may evaluate the ratio of limiting fluorescence yields, r^*_Φ, without resorting to samples with such high probe ratios that the structure of the host lipid would be seriously perturbed.

The model-independent empirical parameter x_0 is useful for characterizing the lateral mobility of excimeric probes. It is readily determined from a monomeric fluorescence yield titration, by use of Eq. 16a.

Provided that the spectral shape of the fluorescence is independent of concentration, it is however not necessary to measure the absolute quantum yields and it is more convenient to use the relative fluorescence yields, defined by $J_M(x) = I_M(x)/x$ and $J_E(x) = I_E(x)/x$, where $I_M(x)$ and $I_E(x)$ are the fluorescence intensities measured at the monomeric and excimeric emission wavelengths, typically 378 and 480 nm for pyrene probes. Because the yields Φ_M and Φ_E are proportional to J_M and J_E, respectively,

$$\Phi_M(x) = \alpha_M J_M(x), \quad \Phi_E(x) = \alpha_E J_E(x) \tag{17}$$

$$\Phi^*_M = \alpha_M J^*_M, \quad \Phi^*_E = \alpha_E J^*_E, \tag{18}$$

where α_M and α_E are constants of the spectrofluorometer used for measuring I_M and I_E. It follows that for any x, the excimer/monomer intensity ratio (r_I) is proportional to the quantum yield ratio:

$$r_I(x) = (\alpha_M/\alpha_E)\, r_\Phi(x). \tag{19}$$

The excimer formation rate may therefore be determined from the excimer/monomer intensity ratios measured at x and at x_0, according to

$$K(x) = [r_I(x)/r_I(x_0)]\, \tau_M^{-1}, \tag{20}$$

which is the result of combining Eqs. 15, 16c, and 19.

Milling crowd model and probe diffusivity

This section shows how the lateral diffusion rate of the probes may be derived from the excimer production rate by the use of the milling crowd model.

Probe molecules, in their excited and ground states (A*, A) are considered to perform a two-dimensional random walk in the membrane leaflet in which they are embedded. The length of each step is L, the average lipid–lipid spacing of the membrane, and spatial exchanges between neighboring probes and lipids take place at an effective frequency f. It is not suggested that such spatial exchanges between neighboring lipid molecules actually occur in membranes, but that the mobility of the molecules, which is limited by the presence of suitable vacancies, can be simulated by an effective exchange of positions at a rate f. The rate of excimer formation depends on x and f and on the probability (p_E) that a nearest neighbor pair (A, A*) form an excimer before the next random step is taken, i.e., in a time interval f^{-1} seconds. That is

$$K(x) = f/n(p_E, x), \tag{21}$$

where $n(p_E, x)$ is the average number of steps taken by the probes before an excimer is formed. The function $n(p_E, x)$ was obtained by computer simulations of the probes' migrations, as described below.

If p_E is unknown, a lower limit for f is given by $p_E = 1$, corresponding to the case in which every nearest neighbor pair becomes an excimer:

$$f_{min} = K(x)n(1, x). \tag{22}$$

With Eqs. 21, 17, 13, and 20 one obtains

$$J_M(x) = J_M^*\left[1 + \frac{f\tau_M}{n(p_E, x)}\right]^{-1} \tag{23a}$$

$$J_E(x) = J_E^*\left[1 + \frac{n(p_E, x)}{f\tau_M}\right]^{-1} \tag{23b}$$

$$\frac{r_1(x)}{r_1(x_0)} = \frac{f\tau_M}{n(p_E, x)}. \tag{24}$$

p_E is in general unknown and must be estimated from the goodness of fit of experimental titration data to Eq. 23 or 24 for different values of p_E. In a companion paper it is shown how an independent estimate of p_E may be obtained by the use of dipyrenyl PC probes (Vauhkonen et al., 1990).

For a molecule which performs a random walk in a plane, taking steps of length L at a rate f, the lateral diffusion coefficient, D, is given by (Berg, 1983),

$$D = fL^2/4. \tag{25}$$

It should be noted that the microscopic (Markovian) definition of D, upon which Eq. 25 is based, assumes that the probes are ideal and is equivalent to the definition of D in Fick's equation for the diffusion in a concentration gradient, as long as D is constant over the region (Einstein, 1906). It is therefore appropriate to compare values of D obtained by use of excimeric probes and FPR experiments.

Milling crowd simulations

To analyze the fluorometric titrations of the present study, we obtained values of $n(p_E, x)$ over a wider range of values of x (0.001–0.3) and with greater precision than previously (Eisinger et al., 1986). The mobility of the probes was simulated by use of the following algorithm.

Lipids and probes form a regular trigonal lattice, so that each probe and lipid has six nearest neighbors. The lattice contains 100 × 100 lattice points and has periodic boundaries. At the beginning of each simulation, m probes are distributed randomly over the lattice points ($m = 10^4x$). Of the m probes, one is chosen at random to be in its excited state (A*), whereas the remaining $m - 1$ probes are in the ground state (A). This means that in an experiment that employs the present analysis the excitation light level must be low enough to ensure that the fraction of probes in the excited state is $<(10^4x)^{-1}$ for all x. All probes then take random steps, in turn, by exchanging places with a randomly chosen nearest neighbor, be it occupied by a lipid or another probe. After each of the m probes has taken one step, the probe-lipid array is searched for the existence of nearest neighbor pairs (A, A*). If none is found, another cycle of random spatial exchanges for all m probes takes place. If one and only one (A, A*) pair is found, an excimer is formed with a probability p_E. Generally, if the A* is found to have q ($q \leq 6$) nearest ground state neighbors (A), an excimer is created with a probability given by $1 - (1 - p_E)^q$. The formation of an excimer ends the simulation and $N(x)$,

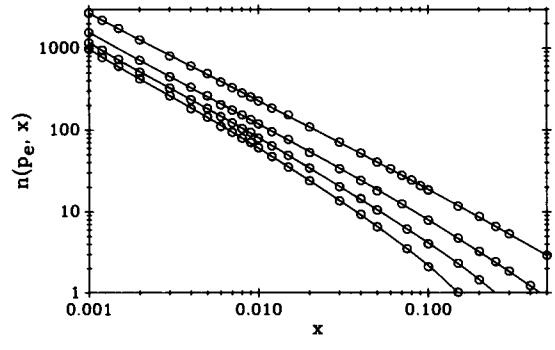

FIGURE 1 The dependence of $n(p_E, x)$, the average number of steps required for the formation of an excimer, as a function of the probe ratio, x. The four curves shown correspond to $p_E = 0.1$, 0.25, 0.5, and 1, reading from top to bottom and are based on computer simulations of random walks of lipid analogue probes in a 100 × 100 regular trigonal lattice of lipids.

the number of stepping cycles which preceded it, is recorded. The A* is then turned into an A and placed in a randomly chosen new position, a new A* is randomly selected and the process is restarted. The values of $N(x)$ for a range of p_E values were averaged for 10,000 random walks for each value of x to obtain $n(p_E, x)$, the average number of steps before excimer formation, and are plotted against x in Fig. 1. The error in $n(p_E, x)$ is ~3% for $x = 0.001$ and considerably smaller for larger values of x.

The average values for $n(x, p_E)$ shown in Fig. 1 were fitted to the following logarithmic polynomial functions by a least squares algorithm:

$$\log_{10} n(1,x) = -3.246 - 7.003y - 5.599y^2 - 2.825y^3 - 0.7190y^4 - 0.07229y^5$$

$$\log_{10} n(0.5,x) = -1.557 - 3.748y - 2.697y^2 - 1.492y^3 - 0.4131y^4 - 0.04462y^5$$

$$\log_{10} n(0.25,x) = -0.523 - 1.610y - 0.2201y^2 - 0.0321y^3$$

$$\log_{10} n(0.1,x) = 0.067 - 1.307y - 0.1177y^2 - 0.0184y^3, \quad (26)$$

where $y = \log_{10} x$. A nonlinear least-squares fitting procedure based on Marquardt's algorithm (Nash, 1979; Marquardt, 1963) was implemented to obtain the best fit values of the various parameters (J_E^*, J_M^*, r_I^*, $f\tau_M$). The program uses the polynomial coefficients shown above to transform the experimental x values into $n(p_E, x)$ for a p_E selected by the user. The experimental yields are then fitted to the appropriate function, Eqs. 23a, 23b or 24, to yield the values of the parameters which minimize the weighted χ^2.

Note that for the analysis of steady-state data, only $n(p_E, x)$, the average number of steps leading to the formation of an excimer, is required, but that the analysis of dynamic fluorescence experiments, e.g., $I_M(t)$, requires knowledge of the frequency distribution of $N(x)$, i.e., of the relative probabilities of random walk lengths. These distributions were obtained along with $n(p_E, x)$ in the milling crowd simulations and are currently being used in the analysis of the concentration dependence of the fluorescence decay rates of monomer and excimer.

EXPERIMENTAL RESULTS

The emission spectra of DMPC unilamellar and multilamellar vesicles containing different amounts of $py_{10}PC$ were measured at temperatures ranging from 5 to 45°C. Typical spectra are shown in Fig. 2. Experimental results for the monomeric and excimeric yields as a function of the probe concentration are shown for three temperatures in Fig. 3, together with the best fit theoretical curves

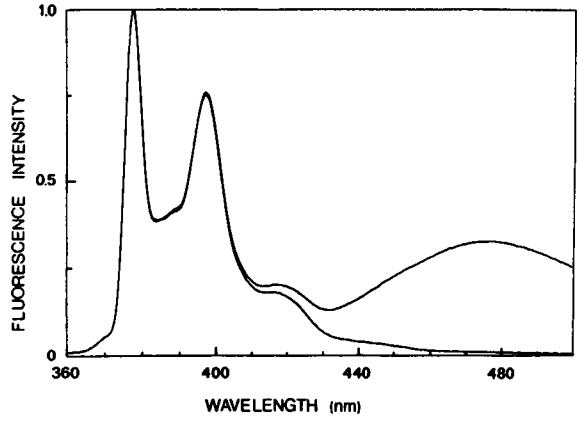

FIGURE 2 The fluorescence spectra of $py_{10}PC$ probes in DMPC unilamellar vesicles for low ($x = 0.001$) and high ($x = 0.1$) probe/lipid ratios. The excitation wavelength was 320 nm and the slits of the excitation and emission monochromators were 4 nm. The intensities of the two emission spectra were normalized at 378 nm, the wavelength of the monomer emission maximum. The broad featureless emission of the excimer is peaked at 480 nm.

according to Eq. 23a and 23b with $p_E = 0.25$. The sensitivity of this analysis to different assumptions for p_E may be gauged by the corresponding values of χ^2: for p_E = 1, 0.5, 0.25, 0.1, the relative values of χ^2 for a DMPC SUV titration at 40°C were 12, 2.9, 1.0, and 1.7, respectively.

Fig. 4 presents the excimer/monomer intensity ratio, $r_I(x)$, as a function of x for the same samples, the data being again fitted with the theoretical curves of Eq. 24, using $p_E = 0.25$. In this case only the value of $r_I^* = r_I(x_0)$

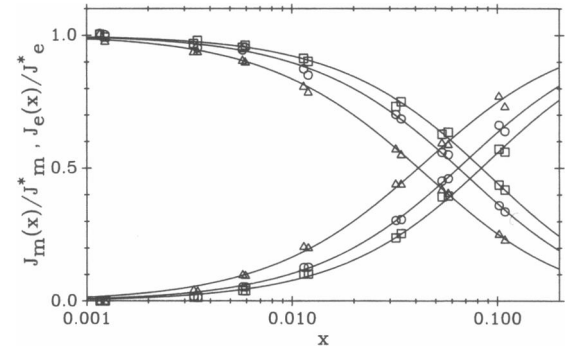

FIGURE 3 The normalized monomer and excimer fluorescence yields of $py_{10}PC$ probes in DMPC SUVs as a function of x, measured at 5°C (□), 25°C (○), and 45°C (△), below and above the phase transition temperature. The experimental data are fitted to Eqs. 23a and 23b, using $p_E = 0.25$, the value which corresponds to the optimum fit to the experimental points. The quality of the fit above and below T_c is comparable, suggesting that the probes are randomly distributed in DMPC in both the fluid and gel phases.

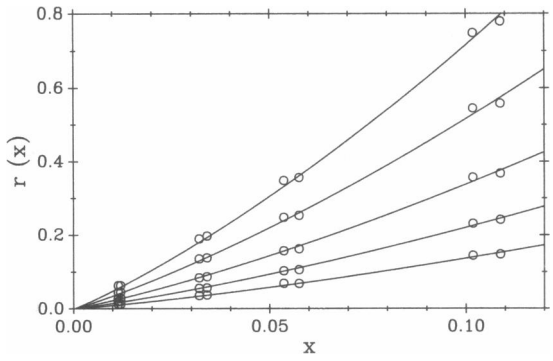

FIGURE 4 The excimer/monomer intensity ratio, $r_I(x)$, of $py_{10}PC$ in DMPC SUVs as a function of the probe ratio, x. The curves (from the bottom) represent the optimum fits of Eq. 24 with $p_E = 0.25$ to experimental points obtained at temperatures of 5, 15, 25, 35, and 45°C.

was optimized, whereas $f\tau_M$ remained fixed at the value obtained by fitting the monomer yields to Eq. 23a.

The empirical fluidity parameter x_0, obtained from the monomer titration data according to Eq. 16c, is shown as a function of temperature in Fig. 5. Note that x_0, a parameter derived from samples with relatively high probe ratios, is nevertheless sensitive to the sharp phase transition at 24°C, showing that the cooperative behavior of the host DMPC bilayer is not seriously perturbed by the presence of the pyrenyl probes. In SUVs, on the other hand, the cooperativity is abolished by the high curvature of the bilayer.

To obtain the probe stepping frequency, f, from the value of $f\tau_M$ which yields the best fit to experiment, τ_M must be known. τ_M of $py_{10}PC$ in DMPC was measured at several temperatures and by making use of the proportionality between lifetime and quantum yield, τ_M was calculated at any temperature from the experimental J^*_M, which were determined along $f\tau_M$, by fitting Eq. 23a to the monomeric yields. From the slope of the Arrhenius plot for f (c.f. Fig. 6), the activation energy for probe diffusion in fluid DMPC was determined to be 8.0 ± 1.5 kcal/mol for MLVs and 7.8 kcal/mol for SUVs.

It should be noted that the Arrhenius plots for SUVs and MLVs differ in the region near the gel-fluid transition temperature, T_c: The pyrenyl probes in multilamellar vesicles display a peak in stepping frequency, whereas f for $py_{10}PC$ in SUVs is a smooth function in the vicinity of T_c. This observation correlates well with the results of other techniques: Among them, ultrasonic relaxation measurements of MLVs (Mitaku et al., 1983) show a peak in the relaxation strength near T_c, which broadens and decreases in amplitude for SUVs; similarly, the peak in the passive sodium permeability near T_c is considerably broader in SUVs than in MLVs (Papahadjopoulos et al., 1973). We suggest that the anomalous increase in f and decrease in x_0 observed by us in the vicinity of the phase transition temperature in MLVs has its origin in the same increase in the fluctuations in the lateral density of the bilayer, which is thought to be responsible for the phenomena described above (Mitaku et al., 1983; Nagle and Scott, 1978).

From the diffusion rate, f, the diffusion coefficient, D, is calculated by means of Eq. 25. Using the average lipid–lipid spacing, L, measured at different temperatures (Janiak et al., 1979), one obtains the values shown in Table 1 and Fig. 7. The figure illustrates the dramatic difference between the effective values of D derived from photobleaching and excimeric probe experiments: while the long-range diffusivity measured by FPR decreases by two orders of magnitude as the host membrane enters the gel phase, the local diffusivity measured in the present study decreases only slightly.

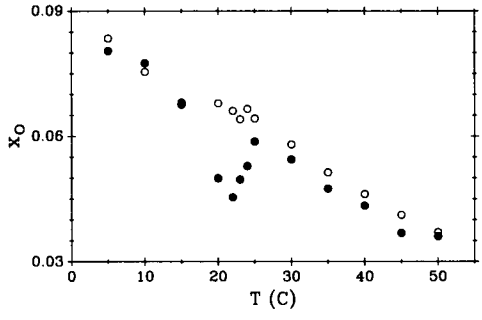

FIGURE 5 The dependence of the critical probe ratio, x_0, defined by Eq. 16a, as a function of temperature. x_0 is the probe ratio for which the rates of excimer formation and monomer decay are the same and may be used as a model-independent measure of the probes' lateral mobility. The open and solid circles refer to SUV and MLV, respectively.

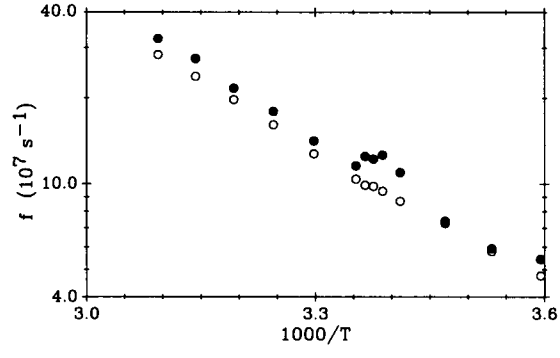

FIGURE 6 Arrhenius plot of the diffusion rate, f, for $py_{10}PC$ in DMPC SUVs and MLVs (*open, solid circles*). Note the apparent increase in f for MLV in the vicinity of the gel-fluid transition temperature, T_c = 24°C.

TABLE 1 Dynamic parameters for $py_{10}PC$ in DMPC multilamellar vesicles for several temperatures, below and above T_c

T	DMPC	τ_M	x_0	f_{min}	D_{min}	f	D
°C	*Phase*	*ns*	%	$10^7\ s^{-1}$	$\mu m^2 s^{-1}$	$10^7\ s^{-1}$	$\mu m^2\ s^{-1}$
5	L_β	200	8.0	2.9	4.5	5.5	6.6
15	P_β	189	6.8	3.8	6.0	7.5	9.0
25	L_α	136	5.9	4.4	7.0	11.7	18
35	L_α	114	4.7	6.0	9.5	18.1	29
45	L_α	97	3.7	8.8	14	27.6	44

f_{min} and D_{min} are the minimum values of these parameters which are consistent with the experimental $J_M(x)$ titration, and are obtained with the assumption, $p_E = 1$ in Eq. 23a. The best fit of these equations to the experimental data is obtained with $p_E = 0.25$, and this is the value used to derive f and D. D was calculated by use of Eq. 25 with $L^2 = 0.62$ nm^2 at 30°C and 0.48 nm^2 at 15°C, the weak temperature dependence of L being taken into account (Janiak et al., 1979).

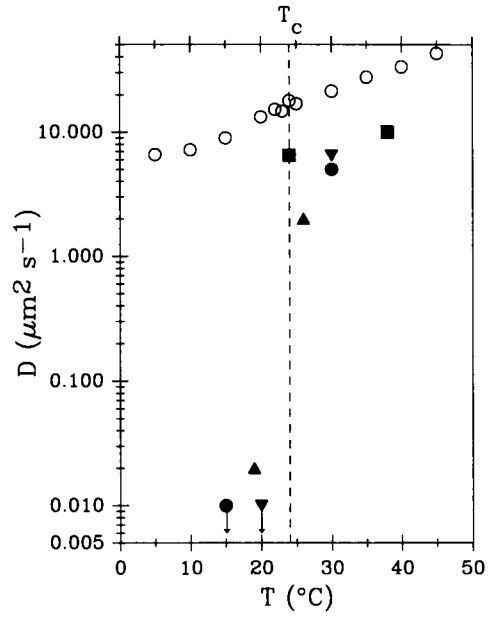

FIGURE 7 The temperature dependence of the lateral diffusion coefficient, D, of lipid analogue probes in DMPC multilamellar vesicles, in the gel and fluid phases. Values obtained in the present study (*open circles*) are compared to the results of photobleaching recovery experiments (*solid symbols*). Above T_c the local diffusion coefficient measured by excimeric probes is three to four times greater than the long-range diffusion coefficients measured by FPR (Tamm, 1988; Alecio et al., 1982; Wu et al., 1977; Smith and McConnell, 1978). Below T_c, however, the D values obtained by FPR are at least two orders of magnitude smaller than those obtained in the present study. For possible reasons for this discrepancy see Discussion.

DISCUSSION

We have presented a general algorithm for determining the local lateral diffusivity of ideally miscible excimeric probes in bilayer systems, specifically from the probe/lipid ratio dependence of their monomeric and excimeric fluorescence yields. The diffusion rate derived from the fluorescence titration data depends on p_E, the probability of a nearest neighbor pair of probes, A and A*, forming an excimer in a time interval f^{-1}. The p_E value which provides the optimum fit between data and theory is selected, but a minimum value for f, f_{min}, and for the lateral diffusion coefficient, D_{min}, is obtained by setting $p_E = 1$.

Whenever extrinsic probes are employed to study a membrane system, their perturbative effect must be considered. Because of the structural similarity of our probes to the matrix lipids and the fact that plots of $r_I(x)$ vs. temperature for x up to 0.1 display a discontinuity at 24°C (data not shown), the DMPC transition temperature, we believe that the probes perturb the bilayers only minimally.

The mobility of fluorescent lipid analogues has been used as a measure of lateral membrane fluidity in several experimental approaches, including FPR, triplet–triplet annihilation (Razi Naqvi et al., 1974; Razi Naqvi, 1974) and the rate of excimer formation as in the present work. The experiments and methods of analysis differ in important respects, particularly in the magnitude of the diffusion distance, which must be taken into account in comparing diffusivities measured by them. We will first compare our results with those obtained previously for DMPC in the liquid crystalline (fluid) phase and then compare results for DMPC in the gel (solid) phase.

Fluid DMPC

Whereas the solubility of pyrenyl probes in gel phase phospholipid bilayers may be problematical, there is little doubt about the miscibility of $py_{10}PC$ in fluid DMPC, as well as other fluid systems (Vauhkonen et al., 1990; Hresko et al., 1986). This is consistent with the excellent fit of $py_{10}PC$ monomer titration data with Eq. 23a, an equation derived on the assumption that the probes mix ideally with the host system and are therefore randomly distributed in it.

The lateral diffusion coefficient of various lipid analogue probes in fluid DMPC has been measured by several investigators using FPR methods. They obtained values of ~2 $\mu m^2 s^{-1}$ at 26°C (Alecio et al., 1982; Fahey and Webb, 1978) and values ranging from 4 to 8 $\mu m^2 s^{-1}$ at 30°C (Tamm, 1988; Kapitza et al., 1984) and from 8 to 18 at 38°C (Derzko and Jacobson, 1980). At these three temperatures our values of D are 19, 24, and 34 $\mu m^2 s^{-1}$, respectively. Whereas the local diffusivities obtained with excimeric probes appear to be several times greater than the FPR values (by a factor of ~4 at 30°C), they are, in

view of the experimental uncertainties of both techniques, considered to be consistent with them. However, the possibility that short-range diffusivities, as measured by bimolecular reaction probes, are systematically higher than the long-range diffusivity measured in FPR experiments can not be excluded.

The mobility of $py_{10}PC$ in fluid DMPC was previously investigated by Galla et al. (1979). However, we analyzed our experiments somewhat differently than these authors. In place of our $n(p_E, x)$ function, they identify the average number of steps leading to excimer formation with a function $n_s(x)$, which was originally derived to estimate the number of steps leading to exciton trapping by a stationary hole in a square array, in the limit of $x \ll 1$ (Montroll, 1969). Because their model requires the coincidence of A* and A, instead of nearest neighbor pair formation followed by excimer production with probability p_E, the stepping frequency derived by them is expected to be smaller by a factor of $\sim(2 \times 6)p_E \approx 3$, assuming $p_E = 0.25$. Here the factor of 2 comes from the fact that their trapping center is stationary, whereas both A and A* are mobile in our model and the factor 6 is the number of nearest neighbors of each probe (hole). If we correct the diffusion frequency of $py_{10}PC$ in DMPC reported by Galla et al., ($4 \times 10^7\ s^{-1}$ for at 30°C), by this factor, their value of D is raised from 6.5 to 19 $\mu m^2\ s^{-1}$, in good agreement with our value of $D = 24\ \mu m^2 s^{-1}$.

Our results can also be compared with the data reported by Hresko et al. (1986), who used the kinetic scheme for diffusion controlled excimer formation developed by Birks et al. (1963) to derive the bimolecular reaction rate $k_{DM}c$ for a 10:90 mixture of $py_{10}PC$/DMPC. With our value of f at 35°C, $18 \times 10^7\ s^{-1}$, and the average number of steps for excimer formation with $x = 0.1$ and $p_E = 0.25$, $n(0.25, 0.1) = 7.87$, we calculate a $k_{DM}c = 2.3 \times 10^7\ s^{-1}$, which is in excellent agreement with the value of $2.7 \times 10^7\ s^{-1}$ reported by Hresko et al. (1986). It should, however, be pointed out that the temperature dependence of this rate obtained by these authors differs from ours, especially in the region of the phase transition, and we cannot identify the origin of this discrepancy at this time.

Gel phase DMPC

Upon cooling below 24°C, DMPC undergoes a cooperative transition from the liquid crystalline (L_α) to the $P_{\beta'}$ or ripple phase, which has been much studied but whose molecular arrangement remains uncertain (Falkovitz et al., 1982; Luna and McConnell, 1977). Further cooling to below 14°C causes DMPC to undergo an additional transition to the $L_{\beta'}$ phase, in which the bilayer is planar and the chains are tilted with respect to its normal. Between 14 and 24°C the bilayers exhibit regular intrabilayer corrugations which give the ripple phase its name: their wavelength depends on water content and has been variously reported to be in the range of 12 to 30 nm (Schneider et al., 1983; Janiak et al., 1979; Luna and McConnell, 1977), whereas their amplitude appears to be between 0.8 and 2.5 nm as determined by x-ray diffraction (Janiak et al., 1979; Stamatoff et al., 1982), but reported to be 4.5 nm according to scanning tunneling microscopy of a freeze fracture replica (Zasadzinski et al., 1988). The $P_{\beta'}$ and the $L_{\beta'}$ phases represent different ways of accommodating the extended acyl chains of DMPC in an area which is smaller than the headgroup. In the fluid or L_α phase this size mismatch is alleviated by the thermally activated introduction of rotational isomers in the acyl chains.

It will be seen below that on the basis of the long-range mobility of lipid analogues measured by FPR, gel phase DMPC appears to be virtually a solid, whereas the present experiments suggest that its local lateral fluidity is only slightly lower than that of fluid DMPC (c.f. Figs. 5–7 and Table 1). This dramatic difference calls for an examination of the assumptions underlying the two experimental approaches.

The dynamic parameters f and x_0 as well as the ratio $r_1(x)$ for all x up to 0.1, are all smooth and continuous functions of temperature, except for a small increase in probe mobility in the fluid-gel transition region (c.f. Figs. 5 and 6 and Results). This suggests that the miscibility of $py_{10}PC$ and DMPC remains high below T_c. The results of Hresko et al. (1986) that the bimolecular reaction rate of the same pyrenyl probes is hardly different above and below T_c, also indicates that extensive probe segregation does not occur in DMPC in passing through the fluid-gel transition. This conclusion is also consistent with the good fit of the fluorometric titration data to Eq. 23a below as well as above T_c (c.f. Fig. 3), although that is a necessary but not sufficient condition for the ideality of probe-lipid mixtures.

These considerations suggest that our analysis of the excimeric probe experiments by use of the milling crowd model is approximately valid for DMPC in the gel phase, although it is shown in a companion paper (Vauhkonen et al., 1990) that this is certainly not the case for other host bilayer systems in the gel phase.

Numerous groups have employed FPR to study the diffusivity of probes in DMPC in its gel phase (Tamm, 1988; Alecio et al., 1982; Wu et al., 1977; Fahey and Webb, 1978; Smith and McConnell, 1978; Schneider et al., 1983). All report lateral diffusion coefficients which are of the order of 0.01 $\mu m^2 s^{-1}$ or at least two orders of magnitude smaller than above the phase transition temperature.

Explanations for this dramatic difference in D mea-

sured by FPR and excimeric probes fall into two categories. The first, drawing an analogy between the effects of cholesterol and excimeric probes on the dynamic properties of the lipid bilayer, argues that $py_{10}PC$ molecules interfere with the ordering of the DMPC acyl chains in the gel phase, inducing local loosening or "fluidization" of the lipid matrix (Somerharju et al., 1985). This would cause the probes to exhibit somewhat greater lateral mobility than the lipid of the unperturbed host system. Related to this is the possibility that nonideal mixing of $py_{10}PC$ and DMPC in the gel phase may result in a nonrandom distribution or clustering of the probes, which would form excimers at an increased rate leading to an overestimation of their mobility. While we cannot at present exclude either of these possibilities, we suggest that the effect produced by them is small in DMPC and that the milling crowd analysis is justified below as well as above T_c.

This conclusion can be tested readily by performing calorimetric measurements of DMPC/$py_{10}PC$ vesicles with different probe ratios. Such experiments are in the planning stage and should eventually provide an estimate of the probe-lipid miscibility and interaction energy. In the meantime we have modified our milling crowd model to allow for nonideal mixing of probe and lipid molecules and are currently performing simulations for a representative set of parameters to investigate the magnitude of the effect which nonrandom probe distributions have on the values of $n(p_E, x)$ and therefore on f and D.

An alternative explanation for the difference in diffusivity measured with bimolecular reaction probes and by photobleaching studies proposes that this difference is related to the 100-fold greater distance (several micrometers) over which the probes must diffuse in an FPR experiment than those traversed by excimeric probes during their excited state lifetime. In traversing such large distances various boundaries or dislocations may present formidable barriers to long-range diffusion, but would have little effect on local probe mobility.

Indeed, freeze fracture electron micrographs of DMPC bilayers in the $P_{\beta'}$ or ripple phase show sharp boundaries, sometimes extending out of the bilayer plane, between regions with different ripple direction (Luna and McConnell, 1977; Zasadzinski et al., 1988; Kapitza et al., 1984). Little is known about the molecular arrangement in these boundary regions but it is possible that diffusion across them is much slower than diffusion within an unperturbed ripple region and that the presence of various dislocations in the gel phase membrane slow long-range diffusion in a manner analogous to that observed for "obstructed diffusion" in which obstacles such as membrane proteins reduce long-range probe mobility (Eisinger et al., 1986; Saxton, 1982). This suggestion is consistent with the observation that the diffusivity of probes in ripple phase DMPC measured by FPR is much lower at high probe concentrations ($x \approx 0.0005$) (Kapitza et al., 1984).

Lateral diffusion constants calculated for lecithin molecules by molecular dynamics simulations also suggest a much closer correspondence of D for the fluid and gel phases than is obtained from the analysis of FPR experiments (Egberts, 1988).

In summary, the intermolecular probe experiments yield diffusion coefficients which are somewhat greater but comparable to those obtained by FPR for fluid DMPC. Both approaches are useful measures of membrane fluidity, but excimeric probes, used in conjunction with quantitative fluorescence microscopy, are expected to provide useful tools for the investigation of fluidity heterogeneities in membranes. Whatever the reason for the disparity between the diffusivities measured by the two techniques for DMPC in the gel phase, the present work provides evidence that the local lateral diffusivity of lipid analogues may be comparable in the fluid and gel phases of DMPC bilayers.

We thank Dr. Istvan Sugar for numerous helpful discussions and Dr. W. Wilson of AT&T Bell Laboratories for the use of his photon counting pulse fluorometer.

This work was supported by a United States Public Health Service award HL21016.

Received for publication 15 June 1989 and in final form 13 October 1989.

REFERENCES

Alecio, M. R., D. E. Golan, W. R. Veatch, and R. R. Rando. 1982. Use of a fluorescent cholesterol derivative to measure lateral mobility of cholesterol in membranes. *Proc. Natl. Acad. Sci. USA.* 79:5171–5174.

Bartlett, G. R. 1959. Phosphorus assay in column chromatography. *J. Biol. Chem.* 234:466–468.

Berg, H. C. 1983. Random Walks in Biology. Princeton University Press, Princeton, NJ. Ch. 1.

Birks, J. B., D. J. Dyson, and I. H. Munro. 1963. Excimer fluorescence. II. Lifetime studies of pyrene solutions. *Proc. R. Soc. Lond. Ser. A.* 275:575–588.

Davenport, L., J. R. Knutson, and L. Brand. 1986. Studies of membrane heterogeneity using fluorescence associative techniques. *Faraday Discuss. Chem. Soc.* 81:81–94.

Derzko, Z., and K. Jacobson. 1980. Comparative lateral diffusion of fluorescent lipid analogues in phospholipid multibilayers. *Biochemistry.* 19:6050–6057.

Egberts, B. 1988. Molecular dynamics simulation of multibilayer membranes. Ph.D. thesis. University of Groningen, Groningen, The Netherlands.

Einstein, A. 1906. Zur Theorie der Brownschen Bewegung. *Ann. Physik.* 19:371–381.

Eisinger, J. 1989. Membrane fluidity and diffusive transport. *In* Fluo-

rescent Biomolecules: Methodologies and Applications. D. M. Jameson and G. D. Reinhart, editors. Plenum Publishing Co., New York. 151–171.

Eisinger, J., J. Flores, and W. P. Petersen. 1986. A milling crowd model for local and long-range obstructed lateral diffusion. Mobility of excimeric probes in the membrane of intact erythrocytes. *Biophys. J.* 49:987–1001.

Fahey, P. F., and W. W. Webb. 1978. Lateral diffusion in phospholipid bilayer membranes and multilamellar liquid crystals. *Biochemistry.* 17:3046–3053.

Falkovitz, M. S., M. Seul, H. L. Frisch, and H. M. McConnell. 1982. Theory of periodic structures in lipid bilayer membranes. *Proc. Natl. Acad. Sci. USA.* 79:3918–3921.

Galla, H. J., W. Hartmann, U. Theilen, and E. Sackmann. 1979. On two-dimensional passive random walk in lipid bilayers and fluid pathways in biomembranes. *J. Membr. Biol.* 48:215–236.

Hresko, R. C., I. P. Sugar, Y. Barenholz, and T. E. Thompson. 1986. Lateral distribution of a pyrene-labeled phosphatidylcholine in phosphatidylcholine bilayers: fluorescence phase and modulation study. *Biochemistry.* 25:3813–3823.

Janiak, M. J., D. M. Small, and G. G. Shipley. 1979. Temperature and compositional dependence of the structure of hydrated dimyristoyl lecithin. *J. Biol. Chem.* 254:6068–6078.

Kapitza, H. G., D. A. Rüppel, H.-J. Galla, and E. Sackmann. 1984. Lateral diffusion of lipids and glycophorin in solid phosphatidylcholine bilayers. The role of structural defects. *Biophys. J.* 45:577–587.

Klausner, R. D., and A. M. Kleinfeld. 1984. Lipid domains in membranes. *In* Cell Surface Dynamics. A. S. Perelson, C. DeLisi, and F. W. Wiegel, editors. Marcel Dekker, Inc., New York. 23–58.

Kremer, J. M. H., J. V. D. Esker, C. Pathmammoharan, and P. H. Wiermsema. 1971. Vesicles of variable diameter prepared by a modified injection method. *Biochemistry.* 16:3932–3935.

Kuo, A. L., and C. G. Wade. 1979. Lipid lateral diffusion by pulsed nuclear magnetic resonance. *Biochemistry.* 18:2300–2308.

Luna, E. J., and H. M. McConnell. 1977. The intermediate monoclinic phase of phosphatidylcholines. *Biochim. Biophys. Acta.* 466:381–382.

Marquardt, D. W. 1963. An algorithm for least-squares estimation of nonlinear parameters. *J. Soc. Ind. Appl. Math.* 11:431–441.

Mitaku, S., T. Jippo, and R. Kataoka. 1983. Thermodynamic properties of the lipid bilayer transition. Pseudocritical phenomena. *Biophys. J.* 42:137–144.

Montroll, E. W. 1969. Random walks on lattices. III. Calculation of first-passage times with application to exciton trapping on photosynthetic units. *J. Math. Phys.* 10:753–765.

Nagle, J. F., and H. L. Scott, Jr. 1978. Lateral compressibility of lipid mono- and bilayers. Theory of membrane permeability. *Biochim. Biophys. Acta.* 513:236–243.

Nash, J. C. 1979. Compact Numerical Methods for Computers: Linear Algebra and Function Minimization. John Wiley & Sons, New York.

Papahadjopoulos, D., K. Jacobson, and S. Nir. 1973. Phase transitions in phospholipid vesicles. Fluorescence polarization and permeability measurements concerning the effect of temperature and cholesterol. *Biochim. Biophys. Acta.* 311:330–348.

Perry, D. G., M. Sassaroli, P. Somerharju, and J. Eisinger. 1988. Intermolecular and intramolecular excimeric probes for determining fluidity of vesicles and membranes. *Biophys. J.* 53:508a. (Abstr.)

Razi Naqvi, K. 1974. Diffusion-controlled reactions in two-dimensional fluids: discussion of measurements of lateral diffusion of lipids in biological membranes. *Chem. Phys. Lett.* 28:280–284.

Razi Naqvi, K., J.-R. Behr, and D. Chapman. 1974. Methods for probing lateral diffusion of membrane components: triplet-triplet annihilation of triplet-triplet energy transfer. *Chem. Phys. Lett.* 26:440–444.

Saxton, M. J. 1982. Lateral diffusion in an archipelago. Effects of impermeable patches on diffusion in a cell membrane. *Biophys. J.* 39:165–173.

Schneider, M. B., W. K. Chan, and W. W. Webb. 1983. Fast diffusion along defects and corrugations in phospholipid Pβ' liquid crystals. *Biophys. J.* 43:157–165.

Sheats, J. R., and H. M. McConnell. 1978. A photochemical technique for measuring lateral diffusion of spin-labeled phospholipids in membranes. *Proc. Natl. Acad. Sci. USA.* 75:4661–4663.

Smith, B. A., and H. M. McConnell. 1978. Determination of molecular motion in membranes using periodic pattern bleaching. *Proc. Natl. Acad. Sci. USA.* 75:2759–2763.

Somerharju, P. J., J. A. Virtanen, K. K. Eklund, P. Vainio, and P. K. J. Kinnunen. 1985. 1-Palmitoyl-2-pyrenedecanoyl glycerophospholipids as membrane probes: evidence for regular distribution in liquid-crystalline phosphatidylcholine bilayers. *Biochemistry.* 24:2773–2781.

Stamatoff, J., B. Feuer, H. J. Guggenheim, G. Tellez, and T. Yamane. 1982. Amplitude of rippling in the Pβ' phase of dipalmitoylphosphatidylcholine bilayers. *Biophys. J.* 38:217–226.

Tamm, L. K. 1988. Lateral diffusion and fluorescence microscope studies on a monoclonal antibody specifically bound to supported phospholipid bilayers. *Biochemistry.* 27:1450–1457.

Vauhkonen, M., M. Sassaroli, P. Somerharju, and J. Eisinger. 1990. Dipyrenyl phosphatidylcholines as membrane fluidity probes. Relationship between intramolecular and intermolecular excimer formation rates. *Biophys. J.* 57:291–300.

Vaz, W. L. C., Z. I. Derzko, and K. A. Jacobson. 1982. Photobleaching measurements of the lateral diffusion of lipids and proteins in artificial phospholipid bilayer membranes. *Cell Surf. Rev.* 8:83–136.

Wu, E. S., K. Jacobson, and D. Papahadjopoulos. 1977. Lateral diffusion in phospholipid multibilayers measured by fluorescence recovery after photobleaching. *Biochemistry.* 16:3936–3941.

Zasadzinski, J. A. N., J. Schneir, J. Gurley, V. Elings, and P. K. Hansma. 1988. Scanning tunneling microscopy of freeze-fracture replicas of biomembranes. *Science (Wash. DC).* 239:1013–1015.